Supplementary information

Piezoelectric-Nanowire Enabled Power Source for Driving Wireless Microelectronics

Sheng Xu, Benjamin J. Hansen and Zhong Lin Wang*

School Materials Science and Engineering, Georgia Institute of Technology, Atlanta, Georgia 30332-0245, USA

* Corresponding author: zlwang@gatech.edu

Figure S1. Characterization of the as grown PZT nanowires. (a) Energy dispersive X-ray spectrum acquired from a single crystal $PbZr_{0.52}Ti_{0.48}O_3$ nanowire in SEM showing its chemical composition. (b) Low magnification TEM image. Scale bar, 500 nm. Upper right is the electron diffraction pattern. Lower left is a corresponding high-resolution TEM image recorded from a PZT nanowire. Scale bar, 4 nm. (c) A dark field image from a PZT nanowire showing the presence of a piezodomain boundary along the length of the nanowire. Scale bar, 200 nm.

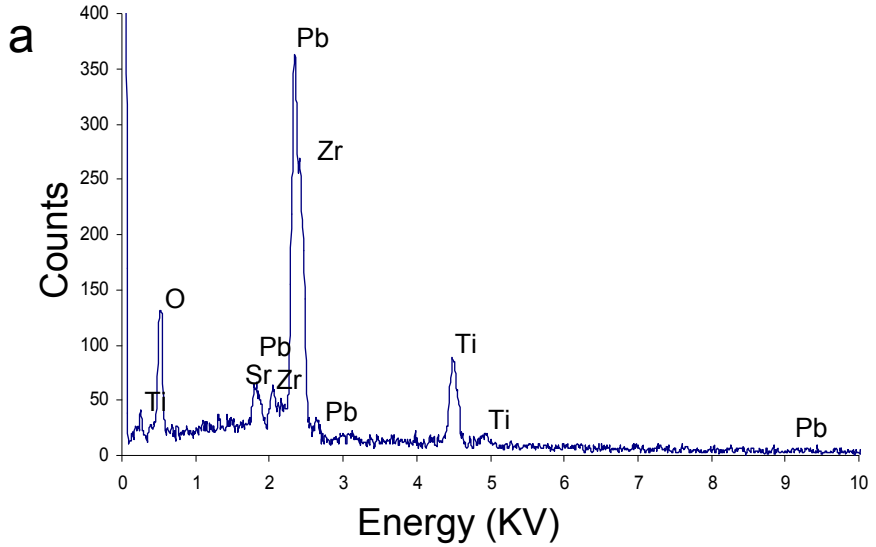

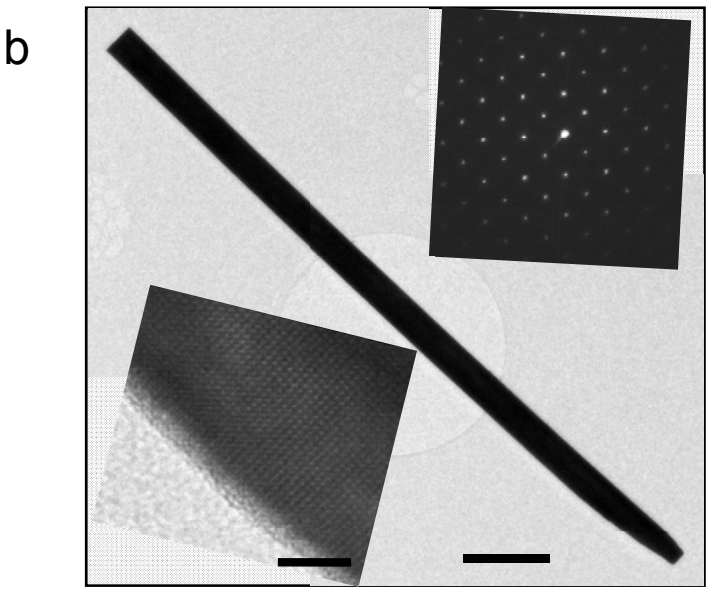

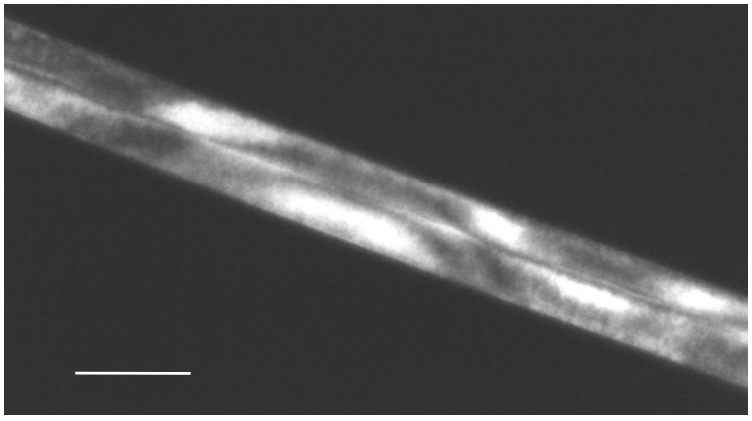

Figure S2. *P-E* ferroelectric hysteresis loop of metal/PZT nanowires/STO capacitors. The loop was obtained at 100 Hz, with P_r and E_c values of about 10 μC/cm^2 and 50 kV/cm, respectively. For the single crystalline PZT here, it is expected that, the E_c should be smaller and the P_r should be larger in comparison with the polycrystalline thin films. In reality, the PZT nanowires grown by low temperature wet chemical method tend to have many oxygen vacancies that would have a pinning effect on the dipole moments. Post high temperature sintering treatment is expected to help improve the performance of the nanowires though. Because leakage current could be large for the relatively porous structure of the nanowire array compared with the dense thin film structures, the maximum applied electric field used in experiment is about 180 kV/cm, which is below saturation. Here if the driving voltage could be increased by infiltration of insulating polymers into the spacing of the nanowires, then the P_{max} and P_r are expected to increase accordingly.

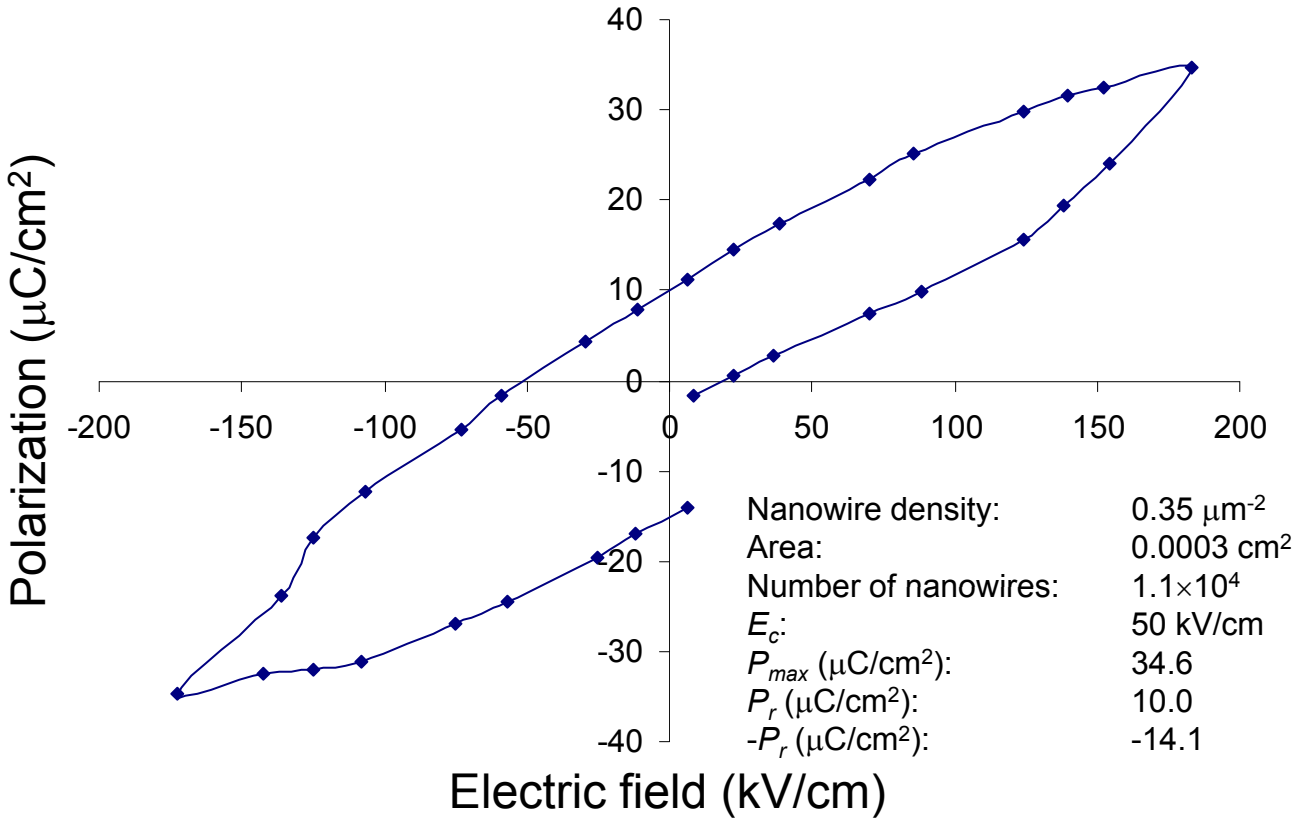

Figure S3. Characterization of the rectifying diodes. (a) I-V characteristics of the two arms of the rectifier. (b) Input signals (navy blue) and output signals (pink) of the rectifier to characterize its performance for rectifying a standard triangle wave.

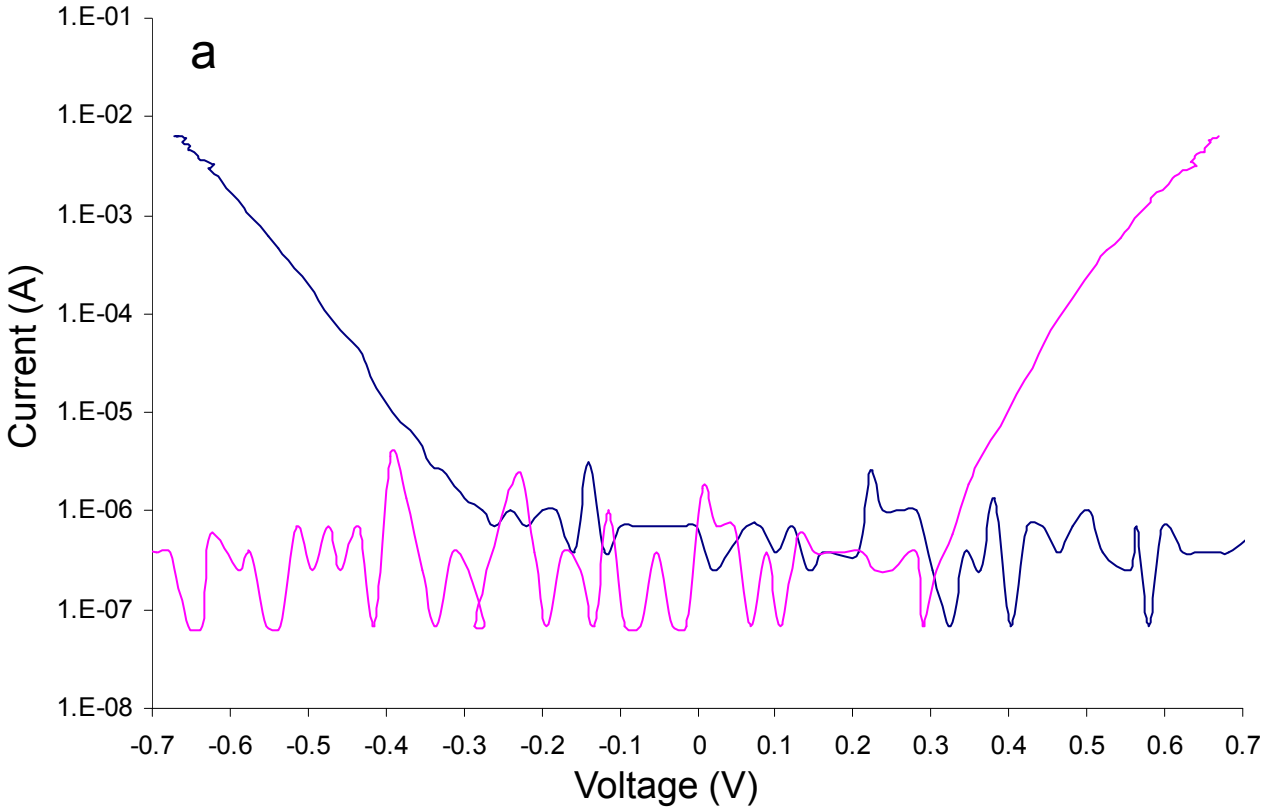

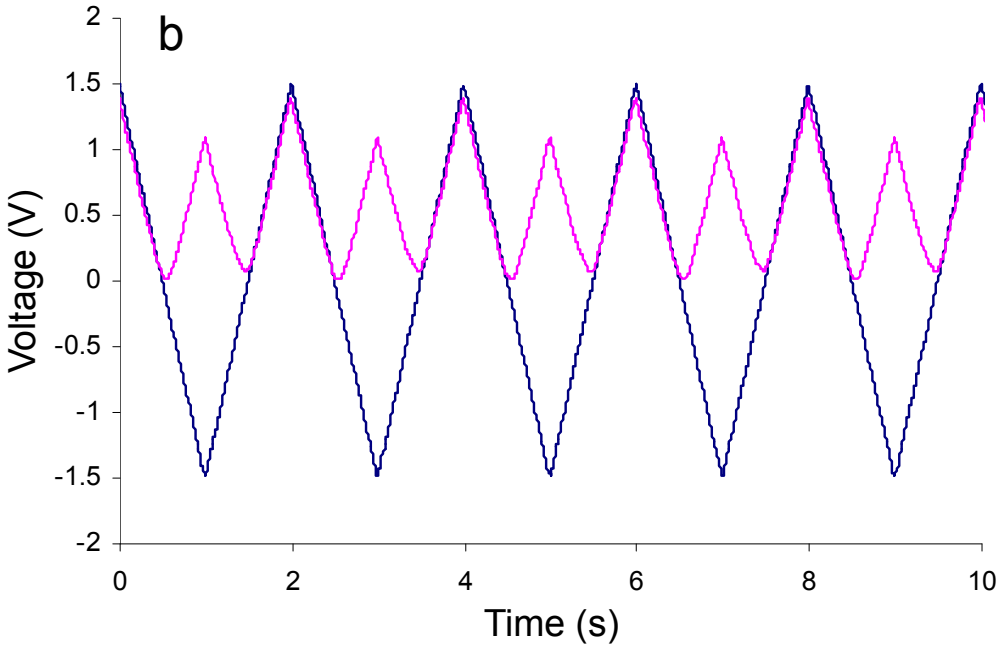

Figure S4. Calculation of the efficiency of the storage circuit. (a) Current peaks for a full cycle of nanogenerator operation when pressed (P) and released (R) after being processed by the rectifier. (b) Integrated injected charges into the capacitors during a cycle of pressing (P) and releasing (R). The calculation result gives the efficiency of the commercial energy storage system used in our study.

a

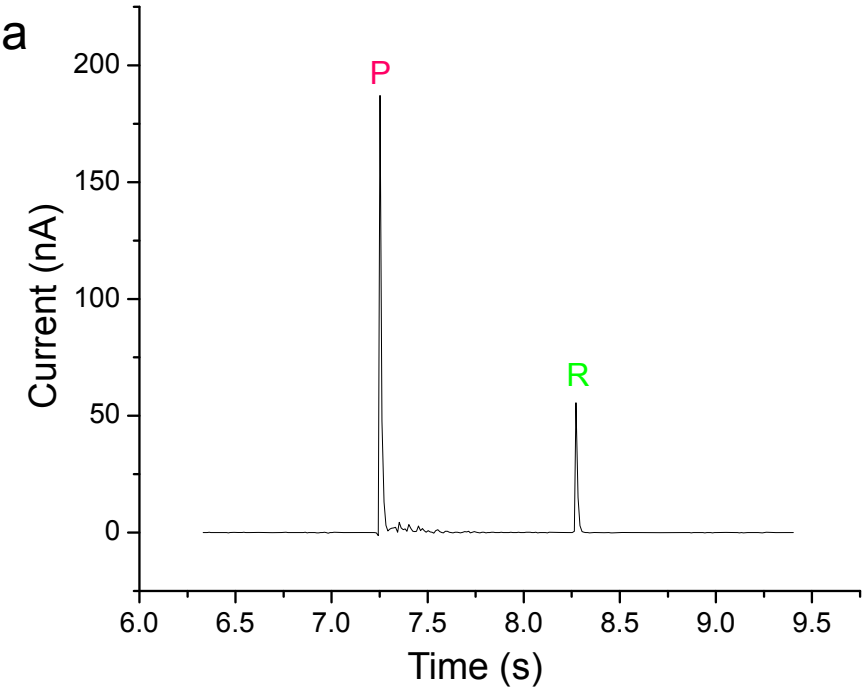

b

	Area (nC)	Width (s)	Center (s)	Height (nA)
P	2.88	0.0193	7.25	187
R	0.75	0.0166	8.27	55.6

Number of cycles: $n = 9 \times 10^4 cycles$

Injected charge per cycle: $2.88 + 0.75 = 3.63\ nC$

Total injected charges: $3.63 \times 9 \times 10^4 nC = 327\ \mu C$

Charges stored in capacitors: $0.42V \times 22\mu F \times 8 = 73.92\mu C$

Efficiency of the storage circuit: $\eta = \frac{73.92}{327} \times 100\% = 23\%$

Figure S5. I-V characteristics of a commercial laser diode used in our experiments.